the representative calcein AM/PI stainings of NGF-treated PC12 (PC12N) cells incubated at 37℃ for 48 h with seed-free unfractionated Aβ1-42 or five fractions (25 μM each). Resultant cell viability for each treatment is shown in the lower half of panel B. Experimental results were analyzed by one-way ANOVA, followed by Dannett's test for posthoc analysis: statistical significance compared with TBS alone (*p<0.001). (C) Dot blot analysis of five fractions (Frs. 1-5). The blots were reacted with A11, 1A9, 2C3, and 4G8. (D) Amplitude AFM images (2 μm x 2 μm) of four fractions (Frs. 2-5). All AFM images were taken on a mica surface.

Figure 3. Immunolabelling characteristics of 1A9, 2C3, A11, 6E10 and 4G8 in human brains. Typical AβO immunolabelling is observed in diffuse plaques (arrow) and the perikaryon of pyramidal neurons (arrow head) as dense granules (A and C) or diffuse staining (B) in AD brains (400X): 1A9 (1:50, panel A), 2C3 (1:50, panel B), and A11 (1:250, panel C). In control brains (D), 1A9 disclosed small granular intraneuronal staining in isolated clusters of pyramidal neurons (400X). (E) Diffuse intraneuronal staing is a characteric feature of control brains (A11, 1:250; 400X). (F) 1A9-positive granules were often observed in dendrires (⊔) in AD brains (400X). (G-H) 4G8 (1:100) and 6E10 (1:100) immunoreactivities were also observed in neurons

(arrow head) and diffuse plaques (arrow) of AD brains, respectively (400X). (I-K) Determinations of number of intraneuronal AβO immunolabelling in human brains: 1A9 (panel I), 2C3 (panel J), and A11 (panel K). Designations used herein were as follows: Granular, dense granule staining; Diffuse, diffuse staining; None, no staining; NC, normal control; AD, Alzheimer's disease. Experimental results of staining pattern were analyzed by one-way ANOVA, followed by Dannett's test for posthoc analysis: statistical significance compared with NC (*p<0.01, **p<0.001).

Figure 4. Cell uptake of neurotoxic AβOs. (A) SH-SY5Y cells were exposed to Fluor™ 488 alone, 5 μM HiLyte Fluor™ 488-labeled AβMs or AβOs (green) at 37℃ for 10, 30, and 180 min. AβMs: 10 kDa-filtrate; AβOs:30 kDa-retentate. Nuclear staining (7-AAD) is shown in red. Vesicular uptake was observed with AβOs, but not with AβMs and Fluor™ 488 alone. (B) The level of LDH released from SH-SY5Y cells treated for the indicated times (0, 3, 6, and 24 h) with 5 μM AβOs. In the case of 5 μM synthetic Aβ42-1 and AβMs, LDH assay was done for 24 h. Each value indicates the percentage level of LDH released following treatment with incubation mixtures relative to the level of LDH released following treatment with Triton X-100. Each column indicates average ± S.D. The p value was determined by one-way

ANOVA, followed by Dannett's test for posthoc analysis: statistical significance compared with AβMs alone (*p<0.05, **p<0.001).

Figure 5. Passive immunization protects Tg2576 mice from memory deficits. Tg2576 mice at 13 months of age in three groups were studied: PBS-treated non-Tg mice, n=14; PBS-treated Tg2576 mice, n=10; 1A9-treated mice, n=13; 2C3-treated mice, n=12. Values indicate the mean ± SEM. (A) Y-maze test. Spontaneous alternation behavior during an 8-min session in the Y-maze task was measured in each group. Results of one-way ANOVA were as follows: F(3, 45)= 2.99, p<0.05, **p<0.05 vs PBS-treated non-Tg mice, #p<0.05 vs PBS-treated Tg2576 mice. (B) Novel object recognition test. The retention session was carried out 24 h after the training. Exploratory preference during a 10-min session in the novel-object recognition test was measured in each group. Results of the two-way ANOVA were as follows: training/retention, F(1, 90)=58.19, p<0.01; animal group, F(3, 90)=6.18, p<0.01; interation of training/retention with animal group, F(3, 90)=7.57, p<0.01; **p<0.01 vs corresponding trained mice. ##p<0.01 vs PBS-treated non-Tg mice, ††p<0.01 vs PBS-treated Tg2576 mice. (C) Swimming-path length during a 60-s session in the water maze test was measured in each group. Results of the two-way ANOVA were as

follows: trial, F(9, 450)=25.51, p<0.01; animal group, F(3, 450)=14.85, p<0.01; interaction of trial with animal group, F(27, 450)= 1.36, p=0.11; **p<0.01 vs PBS-treated non-Tg mice, #p<0.05, ##p<0.01 vs PBS-treated Tg2576 mice. Conditioned fear learning test: context-dependent (D) and cue-dependent (E) freezing times were measured. The results of one-way ANOVA were as follows: context-dependent test, F(3, 45)= 6.19, p<0.01; cue-dependent test, F(3, 45)=5.41, *p<0.05; **p<0.01 vs PBS-treated non-Tg mice, #p<0.05, ##p<0.01 vs PBS-treated Tg2576 mice.

Figure 6. Passive immunization protects Tg2576 mice from synaptic or neuronal degeneration. (**A**) Saline-insoluble, SDS-extractable synaptic proteins were examined by Western blot analysis and probed for PSD95 (1:250), drebrin (DB, 1:100), and synaptophysin (SYP, 1:2000). The p value was determined by one-way ANOVA: *p<0.05. Representive Confocal immunofluorescence microscopy images of Tg2576 mouse brain. Sections of the cortex of the untreated (PBS)-, 1A9-treated, or 2C3-treatedTg2576 mouse brain were immunostained with PSD-95 (Upper part of panel A), Derbrin (DB, Middle part of panel A), synaptophysin (SYP, Lower part of panel A). Scale bar = 30 μm. (**B**) Confocal immunofluorescence microscopy images

of Tg2576 mouse brain. Sections of the hippocampus of the untreated (PBS)-, 1A9-treated, or 2C3-treatedTg2576 mouse brain were immunostained with Fluoro Jade B (1:50000). Scale bar = 100 μm. (**C**) Representive Confocal immunofluorescence microscopy images of AD brain. Sections of the hippocampus of AD brains were immunostained with Fluoro Jade B. Scale bar = 20 μm.

Figure 7. Passive immunization protects Tg2576 mice from accumulation of intraneuronal AβOs. Dot blot immunoassay for A11-immunoreactive AβOs in saline-soluble extracts (**A**), saline-insoluble, SDS-extractable extracts (**B**), and SDS-insoluble, FA-extractable extracts (**C**) obtained from untreated, 1A9-treated, or 2C3-treated mice (30 μg of total extracted brain protein per dot). Results from densitometric imaging of these same samples. The line indicates the mean of each set. The p value was determined by one-way ANOVA: $*p<0.05$, $**p<0.001$. (**C**) Confocal immunofluorescence microscopy images of Tg2576 mouse brain. Sections of the hippocampus of the Tg2576 mouse brain were doubly immunostained with 7-AAD (red, 1:50) and anti-A11 antibody (green, 1:250). Scale bar = 10 μm.

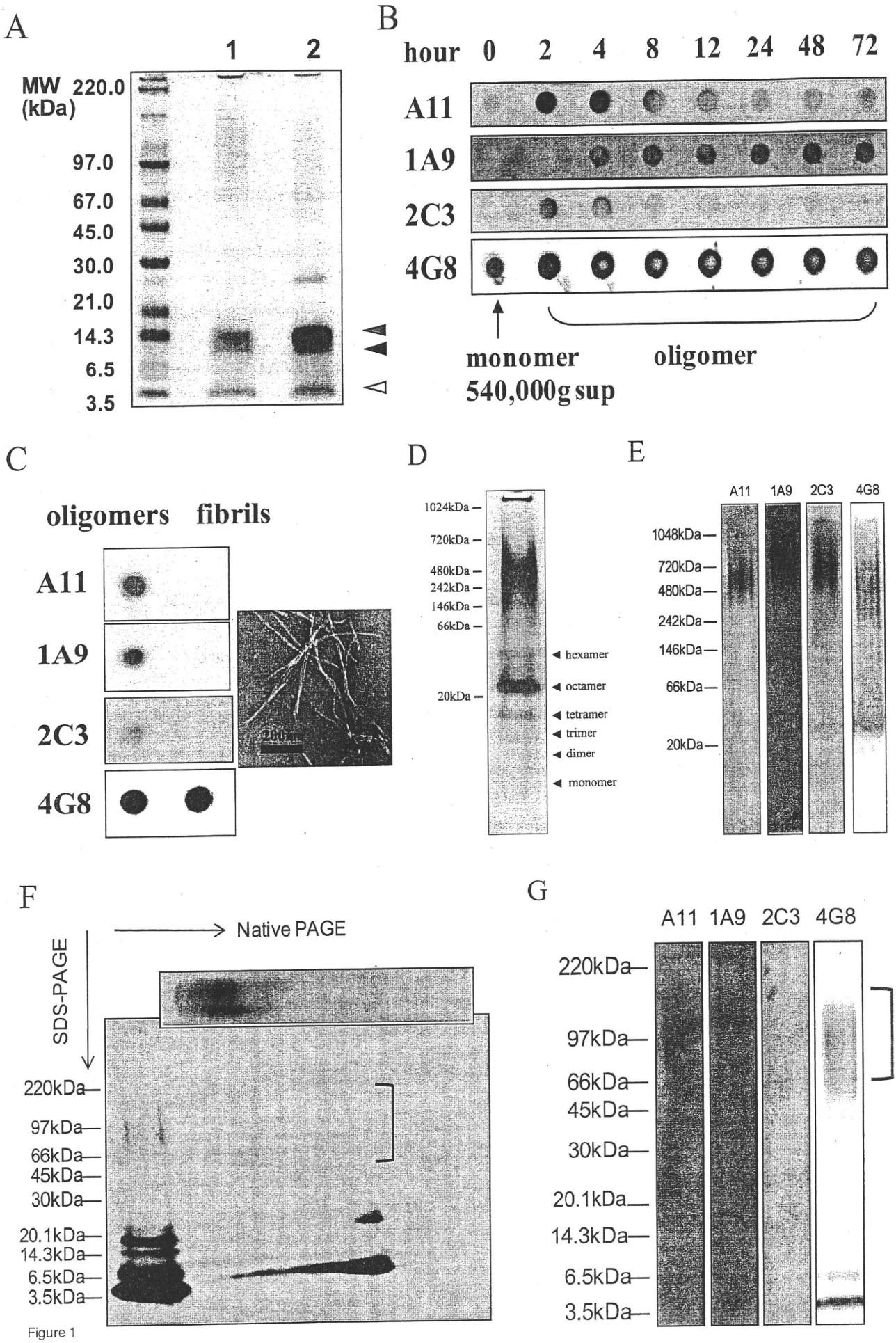
A
1
2
MW (kDa)
220.0
97.0
67.0
45.0
30.0
21.0
14.3
6.5
3.5
B
hour 0 2 4 8 12 24 48 72
A11
1A9
2C3
4G8
monomer
oligomer
540,000g sup
C
oligomers fibrils
A11
1A9
2C3
4G8
200nm
D
1024kDa
720kDa
480kDa
242kDa
146kDa
66kDa
20kDa
hexamer
octamer
tetramer
trimer
dimer
monomer
E
A11 1A9 2C3 4G8
1048kDa
720kDa
480kDa
242kDa
146kDa
66kDa
20kDa
F
Native PAGE
SDS-PAGE
220kDa
97kDa
66kDa
45kDa
30kDa
20.1kDa
14.3kDa
6.5kDa
3.5kDa
G
A11 1A9 2C3 4G8
220kDa
97kDa
66kDa
45kDa
30kDa
20.1kDa
14.3kDa
6.5kDa
3.5kDa

Figure 1

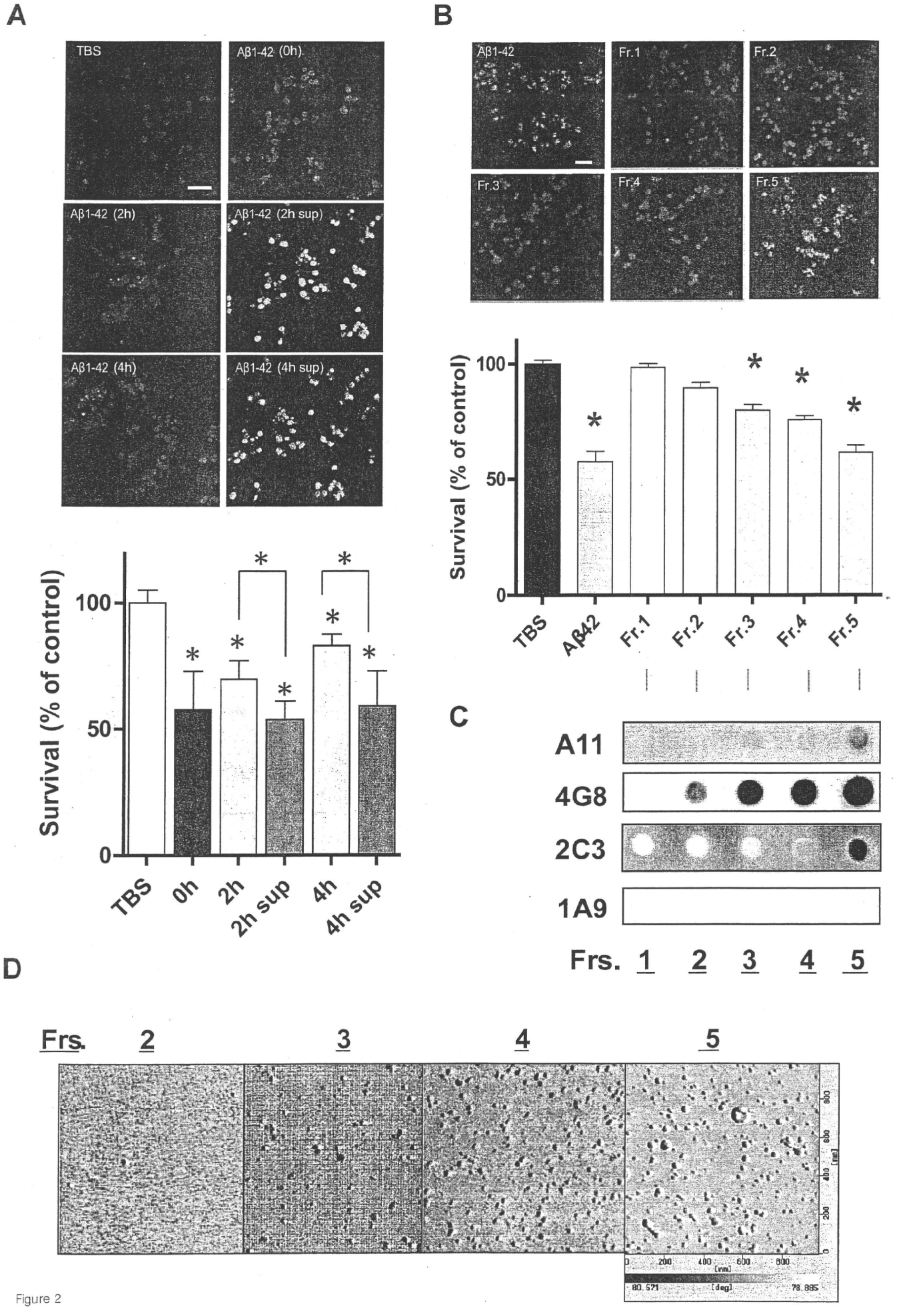
A
TBS
Aβ1-42 (0h)
Aβ1-42 (2h)
Aβ1-42 (2h sup)
Aβ1-42 (4h)
Aβ1-42 (4h sup)
Survival (% of control)
100
50
0
TBS
0h
2h
2h sup
4h
4h sup
B
Aβ1-42
Fr.1
Fr.2
Fr.3
Fr.4
Fr.5
Survival (% of control)
100
50
0
TBS
Aβ42
Fr.1
Fr.2
Fr.3
Fr.4
Fr.5
C
A11
4G8
2C3
1A9
Frs. 1 2 3 4 5
D
Frs. 2 3 4 5

Figure 2

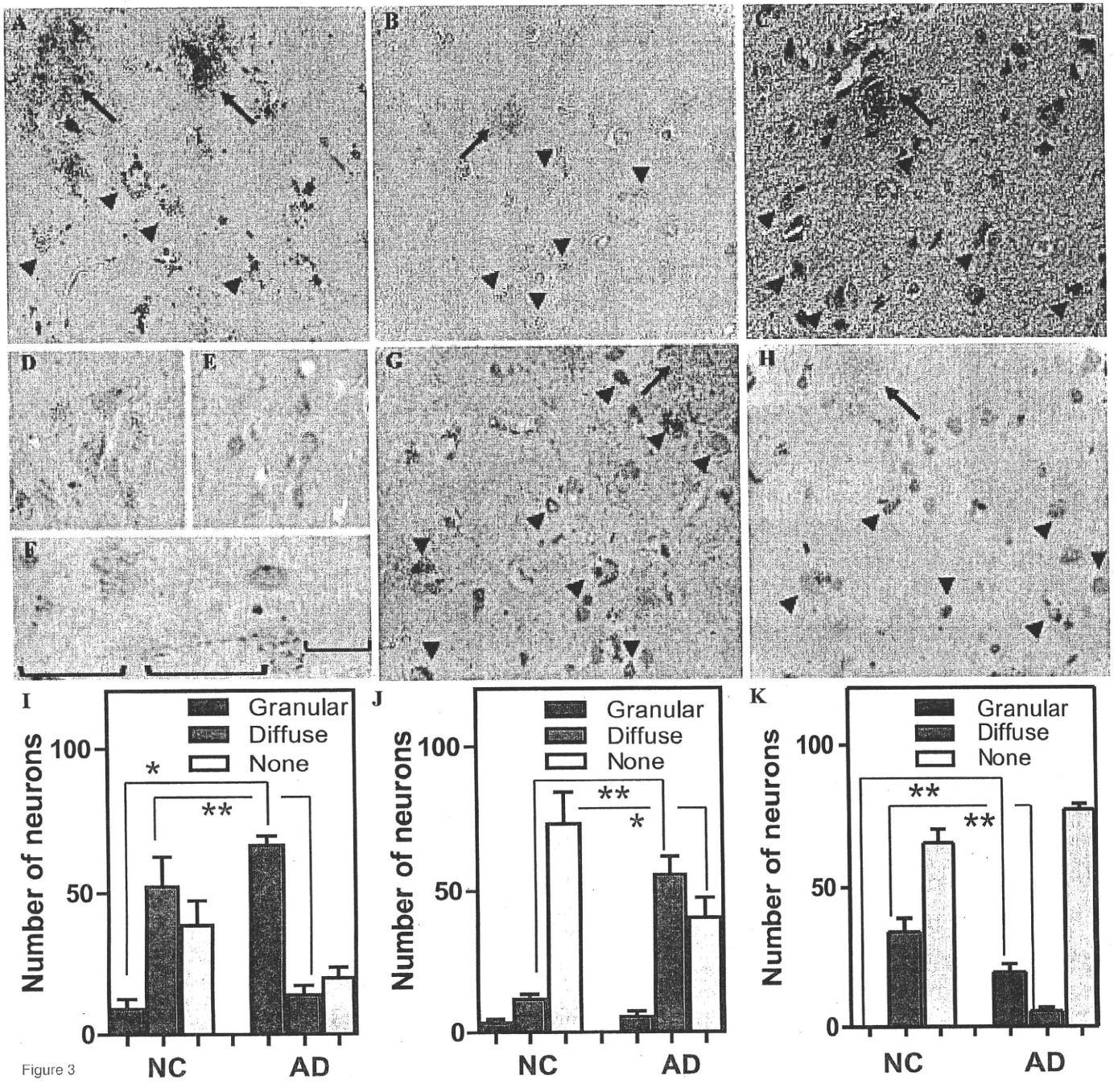
A
B
C
D
E
F
G
H
I
Granular
Diffuse
None
Number of neurons
100
50
0
*
**
NC
AD
J
Granular
Diffuse
None
Number of neurons
100
50
0
**
*
NC
AD
K
Granular
Diffuse
None
Number of neurons
100
50
0
**
**
NC
AD

Figure 3

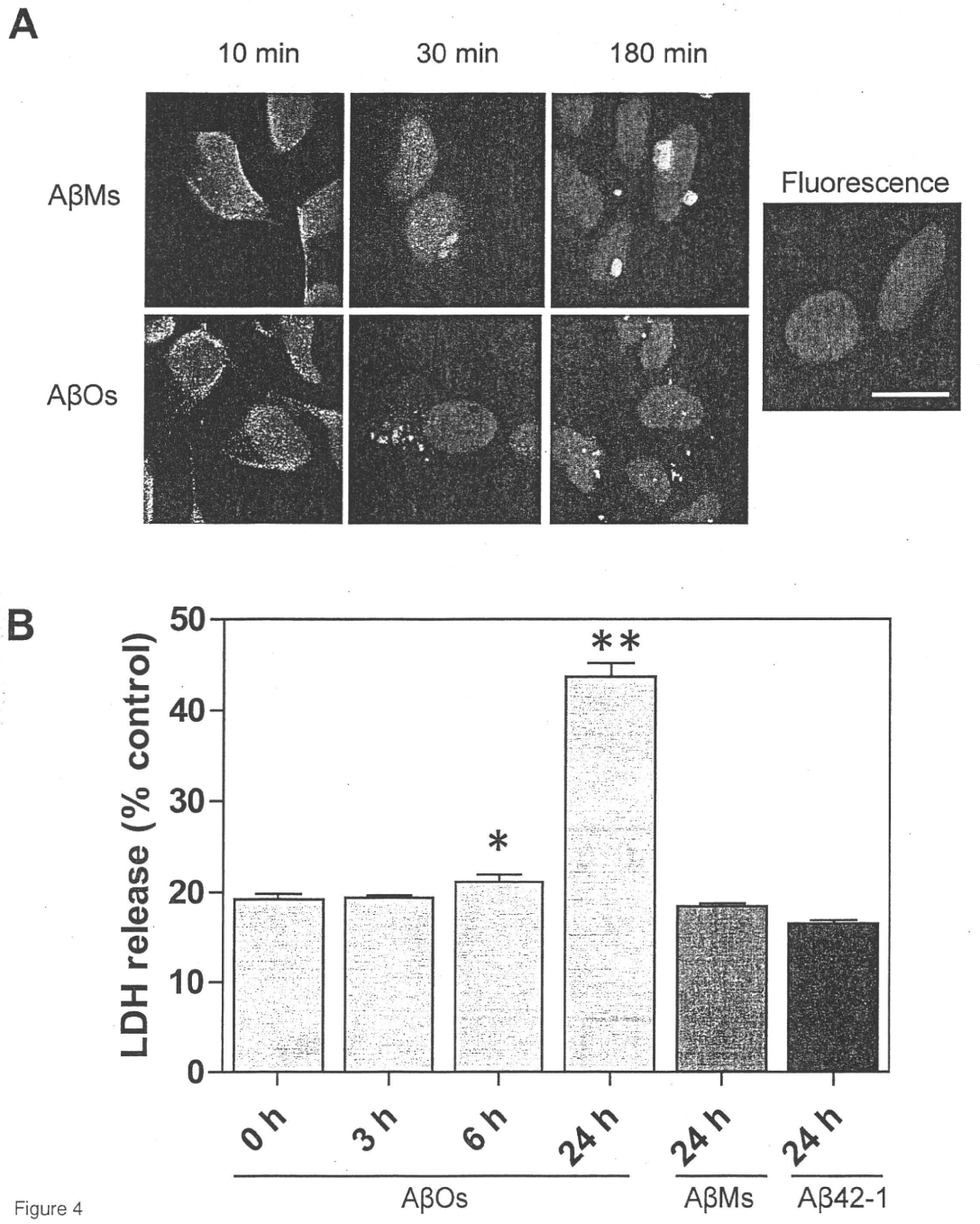
A
10 min
30 min
180 min
AβMs
AβOs
Fluorescence
B
LDH release (% control)
50
40
30
20
10
0
**
*
0 h
3 h
6 h
24 h
24 h
24 h
AβOs
AβMs
Aβ42-1

Figure 4

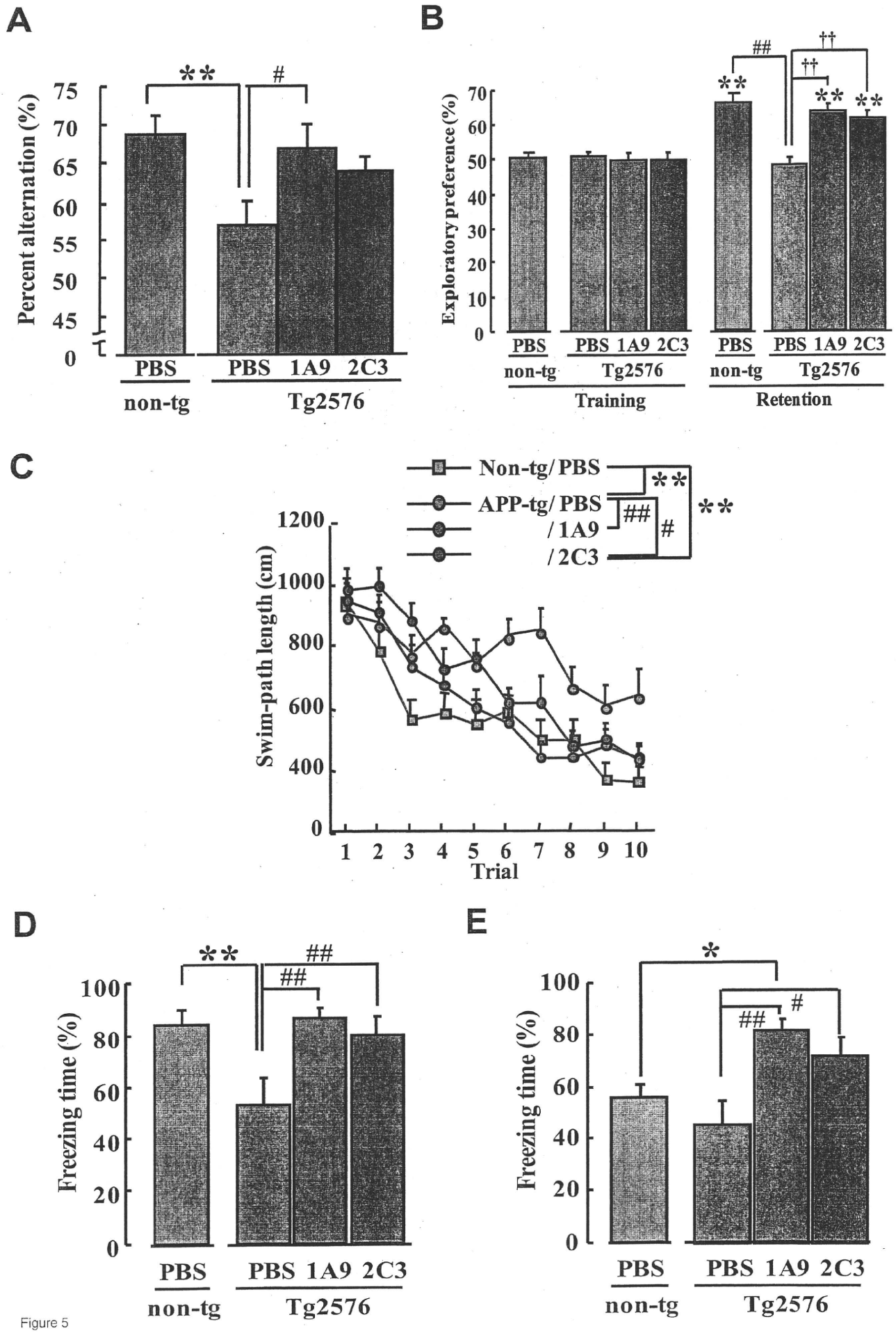
A
Percent alternation (%)
75
70
65
60
55
50
45
0
**
#
PBS
PBS 1A9 2C3
non-tg
Tg2576
B
Exploratory preference (%)
70
60
50
40
30
20
10
0
##
††
††
**
**
**
PBS
PBS 1A9 2C3
PBS
PBS 1A9 2C3
non-tg
Tg2576
non-tg
Tg2576
Training
Retention
C
Non-tg/PBS
APP-tg/PBS
/1A9
/2C3
**
##
#
**
Swim-path length (cm)
1200
1000
800
600
400
0
1 2 3 4 5 6 7 8 9 10
Trial
D
Freezing time (%)
100
80
60
40
20
0
**
##
##
PBS
PBS 1A9 2C3
non-tg
Tg2576
E
Freezing time (%)
100
80
60
40
20
0
*
#
##
PBS
PBS 1A9 2C3
non-tg
Tg2576

Figure 5

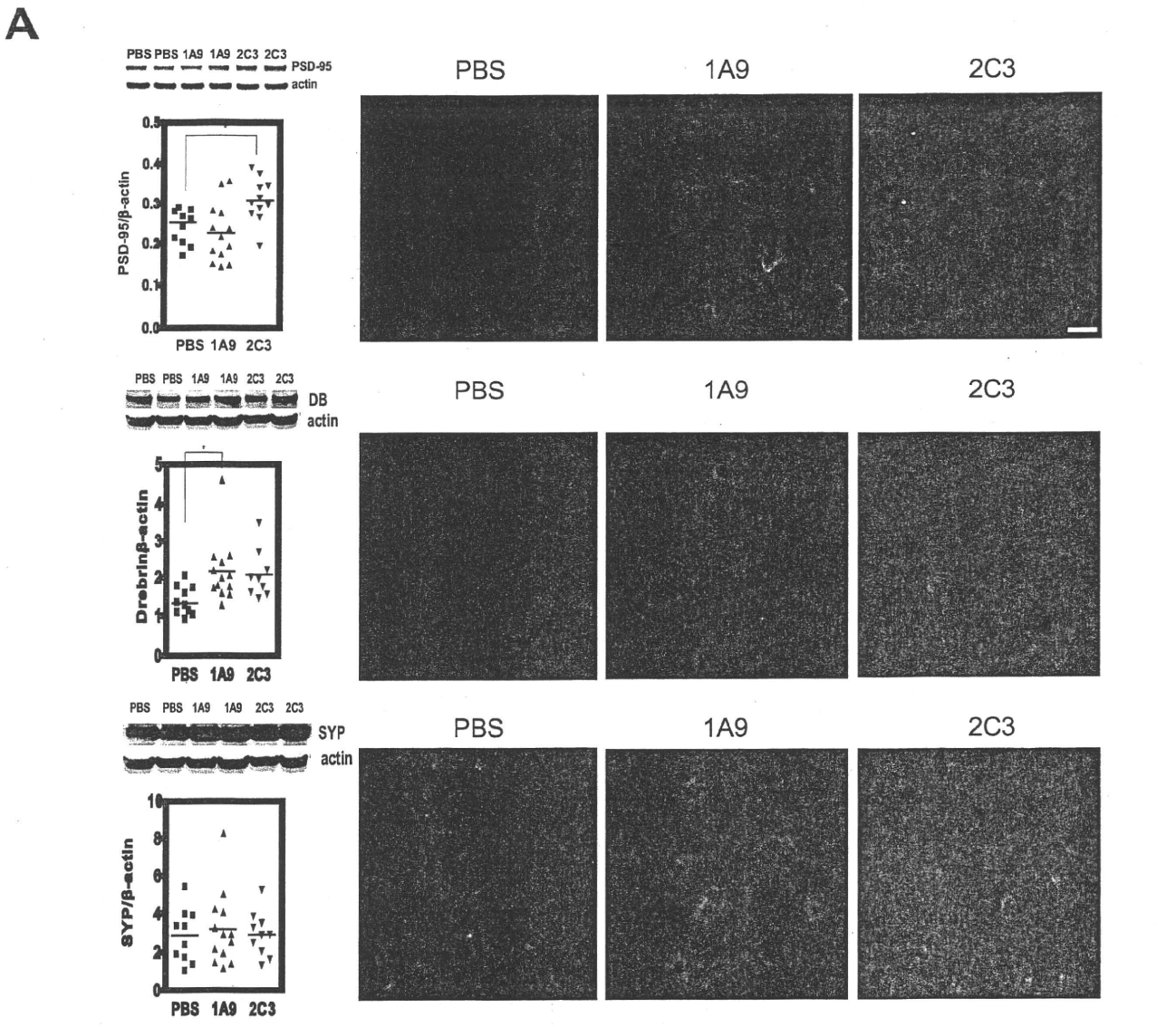
A
PBS PBS 1A9 1A9 2C3 2C3
PSD-95
actin
PSD-95/β-actin
PBS 1A9 2C3
DB
Drebrinβ-actin
SYP
SYP/β-actin
PBS
1A9
2C3
B
100um
C
2C3
FJB
Merge
AD
1A9

Figure 6

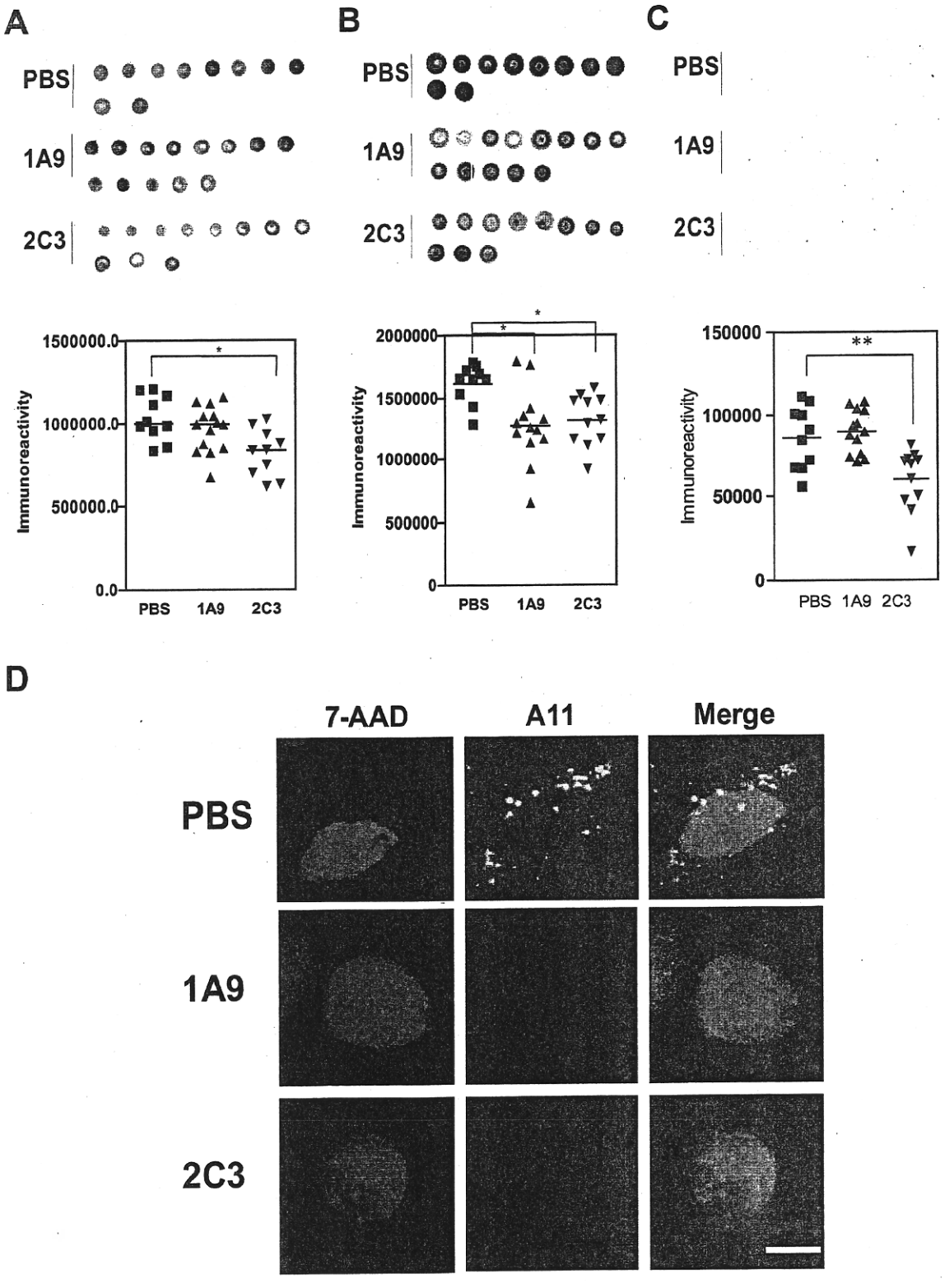
A
PBS
1A9
2C3
B
PBS
1A9
2C3
C
PBS
1A9
2C3
Immunoreactivity
1500000.0
1000000.0
500000.0
0.0
PBS 1A9 2C3
2000000
1500000
1000000
500000
0
150000
100000
50000
*
**
D
7-AAD
A11
Merge
PBS
1A9
2C3

Figure 7

Biochemical and Biophysical Research Communications 402 (2010) 54–58

Contents lists available at ScienceDirect

Biochemical and Biophysical Research Communications

journal homepage: www.elsevier.com/locate/ybbrc

Potent inhibitors of amyloid β fibrillization, 4,5-dianilinophthalimide and staurosporine aglycone, enhance degradation of preformed aggregates of mutant Notch3

Keikichi Takahashi, Kayo Adachi [1], Shohko Kunimoto [1], Hideaki Wakita [1], Kazuya Takeda *[,1], Atsushi Watanabe *[,1]

Department of Vascular Dementia Research, National Institute for Longevity Sciences, National Center for Geriatrics and Gerontology (NCGG), Aichi, Japan

ARTICLE INFO

Article history:
Received 14 September 2010
Available online 1 October 2010

Keywords:
CADASIL
Vascular dementia
Notch3
Protein aggregation
Low-molecular compound

ABSTRACT

Cerebral autosomal dominant arteriopathy with subcortical infarcts and leukoencephalopathy (CADASIL) is caused by mutations in human *NOTCH3*. We have recently reported that mutant Notch3 shows a greater propensity to form aggregates, and these aggregates resist degradation, leading to accumulation in the endoplasmic reticulum (ER). In this study, we searched for low-molecular compounds that decrease the amount of mutant Notch3 aggregates. Using a cell-based system, we found that degradation of preformed mutant aggregates was enhanced by treatment with either 4,5-dianilinophthalimide (DAPH) or staurosporine aglycone (SA), both of which inhibit amyloid β (Aβ) fibrillization. Regarding other low-molecular compounds interacting with Aβ fibrils, thioflavin T (ThT) also enhanced the clearance of mutant Notch3. These findings suggest that DAPH, SA, and ThT are potent reagents to dissociate the preformed aggregates of mutant Notch3 by disruption of intermolecular contacts of misfolded proteins. Our study may provide the basis for the development of a pharmacological therapy for CADASIL.

1. Introduction

Cerebral autosomal dominant arteriopathy with subcortical infarcts and leukoencephalopathy (CADASIL) is a hereditary small vessel disease causing recurrent subcortical ischemic strokes and vascular dementia [1–3]. The pathological hallmarks of the disorder are degeneration of vascular smooth muscle cells (VSMCs) and the abnormal accumulation of granular osmiophilic material (GOM) [4,5]. CADASIL is caused by missense mutations and small deletions in *NOTCH3* [6,7], and the extracellular domain of Notch3 is a constituent of GOM [8]. Although the formation of GOM is considered to be involved in the disease process, the molecular mechanisms by which Notch3 mutations lead to vascular degeneration remain unclear [9–16]. Recently, we have shown that mutant Notch3 is more prone to form aggregates that are accumulated in the endoplasmic reticulum (ER) and is considerably resistant to ER-associated degradation (ERAD) than wild-type Notch3 [17]. These findings indicate that the cytotoxic effects of mutant Notch3 may be related to the formation and accumulation of mutant aggregates in the ER.

In the present study, we searched for low-molecular compounds that efficiently degrade the preformed aggregates of mutant Notch3. Using tetracycline (Tet)-on inducible stable cell lines, we found that the degradation of preformed mutant aggregates was facilitated by treatment with 4,5-dianilinophthalimide (DAPH) and staurosporine aglycone (SA), which inhibit amyloid β (Aβ) fibrillization [18,19]. Furthermore, thioflavin T (ThT), which interacts with Aβ fibrils and senile plaques [20], also accelerated the clearance of mutant Notch3 aggregates. These findings may invigorate hope for a pharmacological therapy of CADASIL patients.

Abbreviations: CADASIL, cerebral autosomal dominant arteriopathy with subcortical infarcts and leukoencephalopathy; ER, endoplasmic reticulum; DAPH, 4,5-dianilinophthalimide; SA, staurosporine aglycone; Aβ, amyloid β; ThT, thioflavin T; VSMCs, vascular smooth muscle cells; GOM, granular osmiophilic material; ERAD, ER-associated degradation; Tet, tetracycline; TUDCA, tauroursodeoxycholic acid; 4PBA, 4-phenylbutyric acid; ThS, thioflavin S; PIB, Pittsburgh compound-B; HEK, human embryonic kidney.

* Corresponding authors. Address: Department of Cognitive Brain Science, Research Institute, National Center for Geriatrics and Gerontology (NCGG), 35 Gengo, Morioka, Obu, Aichi 474-8511, Japan. Fax: +81 562 46 8438.

E-mail addresses: ktakeda@ncgg.go.jp (K. Takeda), watsushi@ncgg.go.jp (A. Watanabe).

[1] Present address: Department of Cognitive Brain Science, Research Institute, National Center for Geriatrics and Gerontology (NCGG), Aichi, Japan.

0006-291X/$ - see front matter © 2010 Elsevier Inc. All rights reserved.
doi:10.1016/j.bbrc.2010.09.105

2. Materials and methods

2.1. Low-molecular compounds

4,5-Dianilinophthalimide (DAPH), staurosporine aglycone (SA), and trehalose were purchased from Sigma. Tauroursodeoxycholic

acid (TUDCA) was from Calbiochem, and thioflavin T (ThT), curcumin, and 4-phenylbutyric acid (4PBA) were from Wako. Thioflavin S (ThS) was from ICN Biomedicals. Tetrahydrocurcumin and resveratrol were kind gifts from Dr. Wakako Maruyama (National Center for Geriatrics and Gerontology). Pittsburgh compound-B (PIB), that is, 2-(4′-methylaminophenyl)-6-hydroxybenzothiazole [21], was a gift from Dr. Seiji Iwasa (Toyohashi University of Technology).

2.2. Stable cell lines

We previously established stable human embryonic kidney (HEK) 293 cell lines in which the expression of Notch3 can be induced using the Tet-on regulatory system (T-Rex system; Invitrogen) [17]. Several cell lines expressing either wild-type or mutant [arginine 133 to cysteine (p.R133C) or cysteine 185 to arginine (p.C185R)] human Notch3 were obtained [17]. The stable cell lines were maintained in DMEM containing 10% fetal bovine serum, 200 μg/ml Zeocin (Invitrogen), and 10 μg/ml blasticidin-S (Invitrogen).

2.3. Western blot analysis

Cells (1.2×10^6) were seeded in six-well plates, treated with 2 μg/ml tetracycline for 24 h, and then cultured in a fresh medium without tetracycline. For treatment of low-molecular compounds, the cells were incubated in the medium containing one of these compounds for 2 days. At indicated times, the cells were harvested and lysed in solution A containing 1% Triton X-100, 0.1 M Tris–HCl (pH 7.4), 0.15 M NaCl, and a protease inhibitor cocktail (Boehringer Mannheim). Lysates (30 μg/lane) were separated on a 7–10% SDS–polyacrylamide gel, and the separated proteins were transferred to a nitrocellulose membrane (Bio-Rad). The membrane was blocked in TBST [10 mM Tris–HCl (pH 7.4), 150 mM NaCl, 0.1% Tween-20] containing 5% nonfat milk and probed using the following the primary and secondary antibodies: a rabbit polyclonal anti-human Notch3 antibody (AbN2, 1 μg/ml) [14,17] and a mouse monoclonal anti-GAPDH antibody (Sigma, 1:2000); a HRP-conjugated goat anti-rabbit antibody (BD Biosciences, 1:3000) and a HRP-conjugated sheep anti-mouse antibody (GE Healthcare, 1:2000). Immunoreactive proteins were detected using Western Lightning chemiluminescence reagents (Perkin Elmer). Protein concentration was determined by micro-BCA assay (Pierce).

2.4. Immunocytochemistry

Cells were cultured in 35-mm Petri dishes coated with poly-L-lysine and fixed in 4% paraformaldehyde in PBS at 4 °C for 10 min. After treatment with 0.2% Triton X-100 for 10 min, cells were blocked with PBS containing 3% fetal bovine serum for 30 min and incubated for 1 h with an anti-Notch3 antibody (AbN2, 1 μg/ml) at room temperature. Cells were washed three times with PBS and incubated for 1 h with a Rhodamine Red-labeled goat anti-rabbit antibody (Molecular Probes) at a 1:1000 dilution in PBS. After three washes in PBS, cells were examined under a light microscope (Olympus). Cells with aggregates were quantified manually by counting cell numbers in phase contrast and immunofluorescence microscopy images and scored as the percentage of the total number of cells.

2.5. Statistical analysis

Data are presented as means ± standard deviation (S.D.). Statistical analysis was performed using unpaired *t*-test (two-tailed) or one-way ANOVA with Dunnett's multiple comparison post hoc test (PRISM version 5.0a; GraphPad Software, La Jolla, CA, USA). Values of $P < 0.05$ were considered significant.

3. Results

3.1. Effects of low-molecular compounds on clearance of mutant Notch3

We established stable HEK293 cell lines in which expression of Notch3 was inducible using the Tet-on regulatory system and showed by pulse-chase analysis and Western blot analysis that the aggregates of mutant Notch3 resisted degradation and accumulated in the ER [17]. Because the expression of Notch3 could be induced and silenced by adding and removing tetracycline, respectively, the degradation rate of Notch3 is easily determined by Western blot analysis. As shown in Fig. 1A, wild-type Notch3 rapidly disappeared within 1 day after silencing its expression, whereas considerable amounts of mutant Notch3 were still detected after 2 days.

Using these cell lines, we searched for low-molecular compounds that facilitated the degradation of the mutant Notch3 aggregates. Previous studies have shown that the chemical

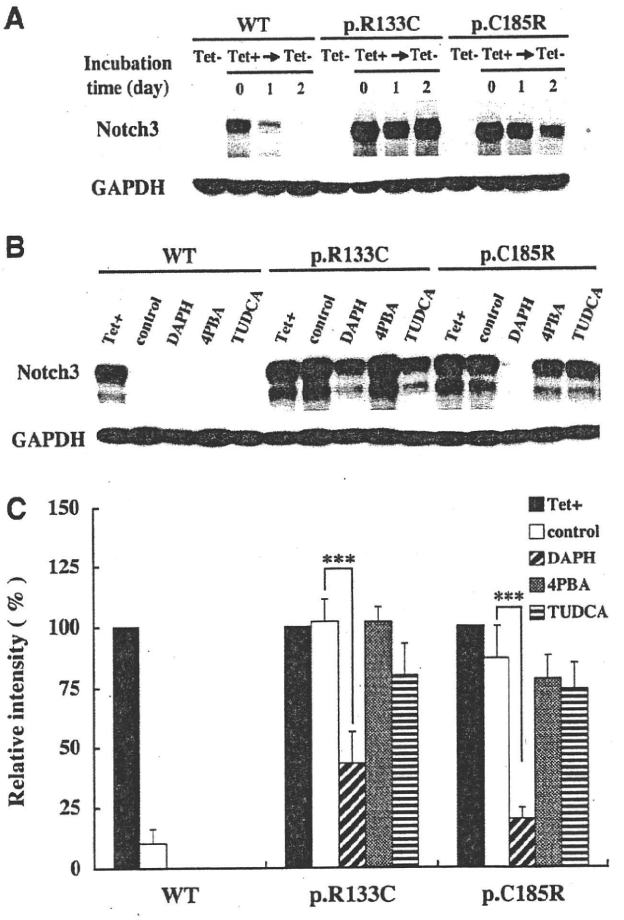

Fig. 1. Effects of low-molecular compounds on degradation of mutant Notch3. (A) Cells were treated with (Tet+) and without (Tet−) 2 μg/ml tetracycline for 24 h and then incubated in the standard medium. The cells were harvested at the indicated times (0–2 days) after the medium change and subjected to Western blot analysis. A representative Western blot is shown. (B) After treatment with 2 μg/ml tetracycline for 24 h (Tet+), cells were incubated in the standard medium with 10 μM DAPH, 20 mM 4PBA or 20 mM TUDCA and without a chemical compound (control) for 2 days. A representative Western blot is shown. (C) Densitometry of the Western blot (B) were performed to estimate relative amounts of wild-type Notch3 and mutant Notch3. Results represent means ± S.D. of data from five experiments and are shown as the percentage of Tet+. ***, $P < 0.001$ relative to untreated cells (control) for each cell line.

chaperones 4PBA and TUDCA modulate the stability of the mutant proteins and inhibit the formation of aggregates [22–24]. In addition, DAPH has been reported to inhibit and reverse the formation of Aβ42 fibrils [18,19]. Therefore, we investigated the effects of these compounds on the clearance of mutant Notch3 aggregates. Stable cells were treated with these compounds for 2 days after stopping the expression of Notch3. As shown in Fig. 1B, treatment with DAPH markedly decreased the amount of mutant Notch3, indicating that this compound effectively enhanced the degradation of mutant Notch3. The amount of mutant Notch3 slightly decreased in cells treated with either 4PBA or TUDCA, although the effect varied among different cell lines expressing mutant Notch3. Quantitative analysis of data showed that only treatment with DAPH resulted in a significant decrease in the amount of mutant Notch3 (Fig. 1C).

3.2. DAPH enhances degradation of mutant Notch3

We determined the effect of DAPH on the clearance of the mutant Notch3 aggregates by immunocytochemical analysis of stable cells using an anti-Notch3 antibody (AbN2). As shown in Fig. 2A, treatment with DAPH significantly decreased the number of cells containing mutant aggregates. Quantitative immunocytochemical analysis revealed that the percentage of cells with mutant Notch3 aggregates to total cells decreased from 35% to 18% for cells expressing the p.R133C mutant and from 33% to 9% for cells expressing the p.C185R mutant following DAPH treatment (Fig. 2B). These results indicate that DAPH enhances the degradation of preformed aggregates of mutant Notch3.

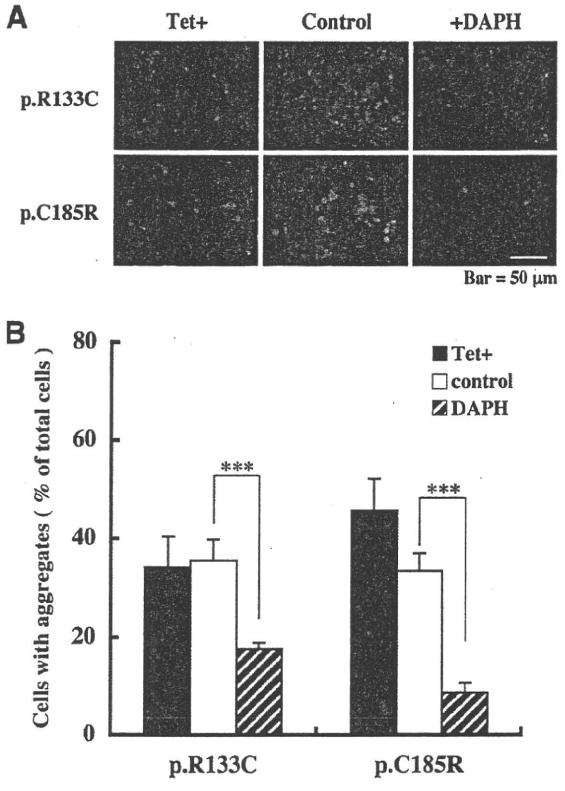

Fig. 2. Effect of DAPH on degradation of preformed mutant aggregates. Cells were treated with 2 μg/ml tetracycline for 24 h (Tet+) and then incubated in the standard medium with 10 μM DAPH or without DAPH (control) for 2 days. (A) Cells were fixed and stained with an anti-Notch3 antibody. Representative photographs are shown. Scale bar, 50 μm. (B) Cells with aggregates were quantified manually by counting cell number 0 day (Tet+) and 2 days after treatment of DAPH. Results represent means ± S.D. of data from five independent images and are shown as the percentage of total number of cells. ***$P < 0.001$ relative to untreated cells (control) of each cell line.

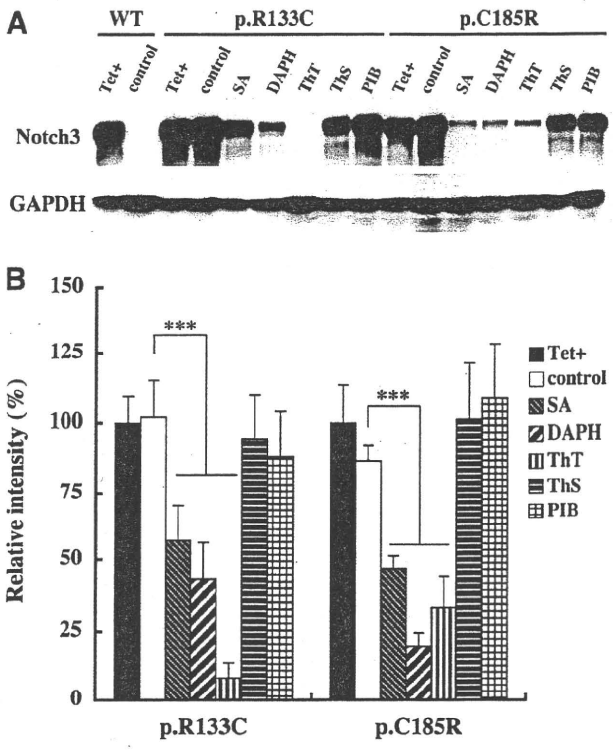

Fig. 3. Effects of Aβ-binding compounds on degradation of mutant Notch3. (A) Cells were treated with 2 μg/ml tetracycline for 24 h (Tet+) and then incubated in the standard medium with 20 μM SA, 10 μM DAPH, 2 μM ThT, 40 μM ThS, or 40 μM PIB and without a chemical compound (control) for 2 days. Cells were lysed and subjected to Western blot analysis. A representative Western blot is shown. (B) Densitometry of the Western blot was performed to estimate relative amounts of mutant Notch3. Results represent means ± S.D. (DAPH $n = 6$, others $n = 4$) and are shown as the percentage of Tet+. ***$P < 0.001$ relative to untreated cells (control) for each cell line.

3.3. Identification of other low-molecular compounds as enhancers of mutant Notch3 degradation

Because DAPH has been reported to inhibit Aβ42 fibrillization [18,19], we determined the effects of other compounds that interact with either Aβ fibrils or amyloid deposits (Fig. 3A and B). SA, an analog of DAPH, was less effective in degrading mutant Notch3 aggregates than DAPH. ThT and ThS, both of which bind the β-sheet structure of amyloid deposits [20], showed their contrasting effects on the degradation of mutant Notch3, the former was more potent than DAPH for the p.R133C mutant, but the latter did not decrease the amount of mutant Notch3. PIB, an amyloid-imaging probe of PET [21], did not degrade mutant Notch3. As shown in Table 1, we also analyzed several compounds including antioxidants (tetrahydrocurcumin and resveratrol), an autophagy inducer (trehalose) [25] and an inhibitor of Aβ aggregation (curcumin) [26]. However, these compounds did not decrease the amount of mutant Notch3, suggesting that the degradation of mutant Notch3 was facilitated by a limited type of inhibitor of Aβ fibrillization.

4. Discussion

Using stable HEK293 cell lines with inducible expression of mutant Notch3, we have shown that the degradation of preformed

Table 1
Summary of effects of low-molecular compounds on degradation of Notch3 aggregates.

Compound	Conc.	Effect	Function
4,5-Dianilinophthalimide (DAPH)	(10 μM)	+++	Inhibitor of Aβ fibrillization
Staurosporine aglycone (SA)	(20 μM)	++	DAPH analog and apoptosis inducer
Thioflavin T (ThT)	(2 μM)	+++	Bind to Aβ and senile plaques
Thioflavin S (ThS)	(40 μM)	–	Bind to Aβ and senile plaques
Curcumin	(30 μM)	–	Inhibitor of Aβ aggregation
PIB	(40 μM)	–	Imaging probe for senile plaques
4-Phenylbutyric acid (4PBA)	(20 mM)	–	Chemical chaperone
Tauroursodeoxycholic acid (TUDCA)	(20 mM)	–	Chemical chaperone
Trehalose	(20 mM)	–	Autophagy inducer
Tetrahydrocurcumin	(20 μM)	–	Antioxidant
Resveratrol	(20 μM)	–	Antioxidant

The effects of chemical compounds were determined as described in Fig. 1C and Fig. 3B. Triple plus (+++) and double plus (++) signs indicate the strong and mild elimination effects on mutant aggregates, respectively. Minus (–) signs represent the insignificant degradation effect on mutant aggregates.

mutant Notch3 aggregates is enhanced by treatment with low-molecular compounds, namely, DAPH and SA, which are novel reagents preventing fibril formation and the neurotoxicity of Aβ42 peptides [18,19]. However, the exact mechanisms of clearing mutant Notch3 aggregates by the inhibitors of Aβ fibrillization are unclear. Previous study using a cell-free system had indicated that DAPH and its analogs change the β-sheet conformation of amyloid fibrils by inhibiting and disrupting the formation of intermolecular contacts, although SA was less potent in inhibiting Aβ fibrillization than DAPH [19]. Because DAPH shows no effect on fiber assembly or disassembly of Tau, α-synuclein and Ure2 [19], the compounds may interact with a specific conformational element of Aβ42 fibrils. Thus, it is likely that DAPH might also recognize a common structure in mutant Notch3 aggregates and disrupt intermolecular contacts of mutant Notch3, resulting in the dissociation and degradation of the aggregates. In addition, ThT showed the ability to degrade aggregates of mutant Notch3. Interestingly, the clearance of mutant Notch3 aggregates was enhanced by the treatment with ThT but not ThS, although both compounds have been known to interact with β-sheet-containing Aβ fibrils and are used as a fluorescence probe to analyze β-sheet formation [20]. Thus, ThT but not ThS may interact with the common element in mutant aggregates that is recognized by DAPH. On the other hand, our previous study has indicated that mutant Notch3 is more prone to form aggregates compared with wild-type Notch3, and mutant aggregates impairs cell proliferation [17]. Therefore, we examined whether DAPH could promote cell proliferation. However, DAPH mildly attenuates cell growth. For this reason, we could not evaluate the exact effect of DAPH on cell proliferation by enhancing the degradation of mutant aggregates in the present study.

Several low-molecular compounds have also been reported to reverse the misfolding of mutant membrane and secretory proteins. 4PBA and TUDCA are chemical chaperones that stabilize protein conformation, improve ER folding capacity, and facilitate the trafficking of mutant proteins [23,24,27]. Trehalose is an autophagy enhancer and inhibits the formation of aggregates and attenuates the toxicity of mutant huntingtin and α-synuclein [25,28]. However, these chemical chaperones or compounds had little effect on the clearance of mutant Notch3, suggesting that the aggregate formation of mutant Notch3 is not reduced by altering the conditions of the ER or inducing autophagy.

Our studies also have shown that the Tet-on inducible cell lines are a useful cellular system for screening the reagents to dissociate the preformed aggregates of mutant Notch3. One of the advantages of this cellular system is that the effects of compounds can be tested under physiological conditions. It has been considered that low-molecular compounds being active in the cell-free system are often inactivate in vivo, because they are not taken up into cells, they interact nonspecifically with other proteins, or they are metabolized into inactive forms. In addition, the efficacy of many compounds is simply determined by quantitative Western blot analysis. Therefore, this cellular system represents an additional tool for studying the processes occurring during the formation of mutant Notch3 aggregates and therapeutic reagents affecting such processes.

In conclusion, using the Tet-on inducible stable cell lines, we screened for low-molecular compounds that efficiently degrade the preformed aggregates of mutant Notch3. By this method, we found that the degradation of preformed mutant aggregates was enhanced by treatment with either DAPH or SA, which inhibits Aβ fibrillization. Our study may be useful for the development of a pharmacological therapy for CADASIL.

Acknowledgments

We thank Ms. Aki Nagasaki and Ms. Mikiko Matsuzaki for excellent technical assistance. This study was supported by the Program for Promotion of Fundamental Studies in Health Science of the National Institute of Biomedical Innovation (NIBIO), a Research Grant for Longevity Sciences (18C-4) from the Ministry of Health, Labour and Welfare, and Grant-in-Aid for Scientific Research [KAKENHI](21790639 and 22500327).

References

[1] E. Tournier-Lasserve, A. Joutel, J. Melki, J. Weissenbach, G.M. Lathrop, H. Chabriat, J.L. Mas, E.A. Cabanis, M. Baudrimont, J. Maciazek, M.A. Bach, M.G. Bousser, Cerebral autosomal dominant arteriopathy with subcortical infarcts and leukoencephalopathy maps to chromosome 19q12, Nat. Genet. 3 (1993) 256–259.
[2] H. Chabriat, K. Vahedi, M.T. Iba-Zizen, A. Joutel, A. Nibbio, T.G. Nagy, M.O. Krebs, J. Julien, B. Dubois, X. Ducrocq, M. Levasseur, P. Homeyer, J.L. Mas, O. Lyon-Caen, E. Tournier-Lasserve, M.G. Bousser, Clinical spectrum of CADASIL: a study of 7 families. Cerebral autosomal dominant arteriopathy with subcortical infarcts and leukoencephalopathy, Lancet 346 (1995) 934–939.
[3] M.M. Ruchoux, C.A. Maurage, CADASIL: cerebral autosomal dominant arteriopathy with subcortical infarcts and leukoencephalopathy, J. Neuropathol. Exp. Neurol. 56 (1997) 947–964.
[4] M.M. Ruchoux, H. Chabriat, M.G. Bousser, M. Baudrimont, E. Tournier-Lasserve, Presence of ultrastructural arterial lesions in muscle and skin vessels of patients with CADASIL, Stroke 25 (1994) 2291–2292.
[5] J.M. Schröder, B. Sellhaus, J. Jörg, Identification of the characteristic vascular changes in a sural nerve biopsy of a case with cerebral autosomal dominant arteriopathy with subcortical infarcts and leukoencephalopathy (CADASIL), Acta Neuropathol. 89 (1995) 116–121.
[6] A. Joutel, C. Corpechot, A. Ducros, K. Vahedi, H. Chabriat, P. Mouton, S. Alamowitch, V. Domenga, M. Cécillion, E. Maréchal, J. Maciazek, C. Vayssiére, C. Cruaud, E.A. Cabanis, M.M. Ruchoux, J. Weissenbach, J.F. Bach, M.G. Bousser, E. Tournier-Lasserve, Notch3 mutations in CADASIL, a hereditary adult-onset condition causing stroke and dementia, Nature 383 (1996) 707–710.

[7] A. Joutel, K. Vahedi, C. Corpechot, A. Troesch, H. Chabriat, C. Vayssiére, C. Cruaud, J. Maciazek, J. Weissenbach, M.G. Bousser, J.F. Bach, E. Tournier-Lasserve, Strong clustering and stereotyped nature of Notch3 mutations in CADASIL patients, Lancet 350 (1997) 1511–1515.
[8] A. Ishiko, A. Shimizu, E. Nagata, K. Takahashi, T. Tabira, N. Suzuki, Notch3 ectodomain is a major component of granular osmiophilic material (GOM) in CADASIL, Acta Neuropathol. 112 (2006) 333–339.
[9] A. Joutel, F. Andreux, S. Gaulis, V. Domenga, M. Cécillion, N. Battail, N. Piga, F. Chapon, C. Godfrain, E. Tournier-Lasserve, The ectodomain of the Notch3 receptor accumulates within the cerebrovasculature of CADASIL patients, J. Clin. Invest. 105 (2000) 597–605.
[10] H. Karlström, P. Beatus, K. Dannaeus, G. Chapman, U. Lendahl, J. Lundkvist, A CADASIL-mutated Notch3 receptor exhibits impaired intracellular trafficking and maturation but normal ligand-induced signaling, Proc. Natl. Acad. Sci. USA 99 (2002) 17119–17124.
[11] M.M. Ruchoux, V. Domenga, P. Brulin, J. Maciazek, S. Limol, E. Tournier-Lasserve, A. Joutel, Transgenic mice expressing mutant Notch3 develop vascular alterations characteristic of cerebral autosomal dominant arteriopathy with subcortical infarcts and leukoencephalopathy, Am. J. Pathol. 162 (2003) 329–342.
[12] N. Peters, C. Opherk, S. Zacherle, A. Capell, P. Gempel, M. Dichgans, CADASIL-associated Notch3 mutations have differential effects both on ligand binding and ligand-induced Notch3 receptor signaling through RBP-Jk, Exp. Cell Res. 299 (2004) 454–464.
[13] A. Joutel, M. Monet, V. Domenga, F. Riant, E. Tournier-Lasserve, Pathogenic mutations associated with cerebral autosomal dominant arteriopathy with subcortical infarcts and leukoencephalopathy differently affect Jagged1 binding and Notch3 activity via the RBP/Jk signaling pathway, Am. J. Hum. Genet. 74 (2004) 338–347.
[14] W.C. Low, Y. Santa, K. Takahashi, T. Tabira, R.N. Kalaria, CADASIL-causing mutations do not alter Notch3 receptor processing and activation, Neuroreport 17 (2006) 945–949.
[15] S. Ihalainen, R. Soliymani, E. Iivanainen, K. Mykkänen, A. Sainio, M. Pöyhönen, K. Elenius, H. Järveläinen, M. Viitanen, H. Kalimo, M. Baumann, Proteome analysis of cultivated vascular smooth muscle cells from a CADASIL patient, Mol. Med. 13 (2007) 305–314.
[16] C. Opherk, M. Duering, N. Peters, A. Karpinska, S. Rosner, E. Schneider, B. Bader, A. Giese, M. Dichgans, CADASIL mutations enhance spontaneous multimerization of *NOTCH3*, Hum. Mol. Genet. 18 (2009) 2761–2767.
[17] K. Takahashi, K. Adachi, K. Yoshizaki, S. Kunimoto, R.N. Kalaria, A. Watanabe, Mutations in *NOTCH3* cause the formation and retention of aggregates in the endoplasmic reticulum, leading to impaired cell proliferation, Hum. Mol. Genet. 19 (2010) 79–89.
[18] B.J. Blanchard, A. Chen, L.M. Rozeboom, K.A. Stafford, P. Weigele, V.M. Ingram, Efficient reversal of Alzheimer's disease fibril formation and elimination of neurotoxicity by a small molecule, Proc. Natl. Acad. Sci. USA 101 (2004) 14326–14332.
[19] H. Wang, M.L. Duennwald, B.E. Roberts, L.M. Rozeboom, Y.L. Zhang, A.D. Steele, R. Krishnan, L.J. Su, D. Griffin, S. Mukhopadhyay, E.J. Hennessy, P. Weigele, B.J. Blanchard, J. King, A.A. Deniz, S.L. Buchwald, V.M. Ingram, Direct and selective elimination of specific prions and amyloids by 4,5-dianilinophthalimide and analogs, Proc. Natl. Acad. Sci. USA 105 (2008) 7159–7164.
[20] G.T. Westermark, K.H. Johnson, P. Westermark, Staining methods for identification of amyloid in tissue, Methods Enzymol. 309 (1999) 3–25.
[21] W.E. Klunk, H. Engler, A. Nordberg, Y. Wang, G. Blomqvist, D.P. Holt, M. Bergström, I. Savitcheva, G.F. Huang, S. Estrada, B. Ausén, M.L. Debnath, J. Barletta, J.C. Price, J. Sandell, B.J. Lopresti, A. Wall, P. Koivisto, G. Antoni, C.A. Mathis, B. Långström, Imaging brain amyloid in Alzheimer's disease with Pittsburgh Compound-B, Ann. Neurol. 55 (2004) 306–319.
[22] G. Bonapace, A. Waheed, G.N. Shah, W.S. Sly, Chemical chaperones protect from effects of apoptosis-inducing mutation in carbonic anhydrase IV identified in retinitis pigmentosa 17, Proc. Natl. Acad. Sci. USA 101 (2004) 12300–12305.
[23] K. Kubota, Y. Niinuma, M. Kaneko, Y. Okuma, M. Sugai, T. Omura, M. Uesugi, T. Uehara, T. Hosoi, Y. Nomura, Suppresive effects of 4-phenylbutyrate on the aggregation of Pael receptors and endoplasmic reticulum stress, J. Neurochem. 97 (2006) 1259–1268.
[24] U. Özcan, E. Yilmaz, L. Özcan, M. Furuhashi, E. Vaillancourt, R.O. Smith, C.Z. Görgün, G.S. Hotamisligil, Chemical chaperones reduce ER stress and restore glucose homeostasis in a mouse model of type 2 diabetes, Science 313 (2006) 1137–1140.
[25] S. Sarkar, J.E. Davies, Z. Huang, A. Tunnacliffe, D.C. Rubinsztein, Trehalose, a novel mTOR-independent autophagy enhancer, accelerates the clearance of mutant huntingtin and α-synuclein, J. Biol. Chem. 282 (2007) 5641–5652.
[26] F. Yang, G.P. Lim, A.N. Begum, O.J. Ubeda, M.R. Simmons, S.S. Ambegaokar, P. Chen, R. Kayed, C.G. Glabe, S.A. Frautschy, G.M. Cole, Curcumin inhibits formation of amyloid β oligomers and fibrils, binds plaques, and reduces amyloid in vivo, J. Biol. Chem. 280 (2005) 5892–5901.
[27] S.F. de Almeida, G. Picarote, J.V. Fleming, M. Carmo-Fonseca, J.E. Azevedo, M. de Sousa, Chemical chaperones reduce endoplasmic reticulum stress and prevent mutant HFE aggregate formation, J. Biol. Chem. 282 (2007) 27905–27912.
[28] M. Tanaka, Y. Machida, S. Niu, T. Ikeda, N.R. Jana, H. Doi, M. Kurosawa, M. Nekooki, N. Nukina, Trehalose alleviates polyglutamine-mediated pathology in a mouse model of Huntington disease, Nat. Med. 10 (2004) 148–154.

Human Molecular Genetics, 2010, Vol. 19, No. 1 **79–89**
doi:10.1093/hmg/ddp468
Advance Access published on October 13, 2009

Mutations in NOTCH3 cause the formation and retention of aggregates in the endoplasmic reticulum, leading to impaired cell proliferation

Keikichi Takahashi[1], Kayo Adachi[1], Kaichi Yoshizaki[1,†], Shohko Kunimoto[1], Raj N. Kalaria[2] and Atsushi Watanabe[1,*]

[1]Department of Vascular Dementia Research, National Institute for Longevity Science, National Center for Geriatrics and Gerontology, Aichi, Japan and [2]Institute for Ageing and Health, Newcastle University, Newcastle upon Tyne NE4 5PL, UK

Received May 28, 2009; Revised and Accepted October 6, 2009

Mutations in the human *NOTCH3* gene cause cerebral autosomal-dominant arteriopathy with subcortical infarcts and leukoencephalopathy (CADASIL), but the pathogenic mechanisms of the disorder remain unclear. We investigated the cytotoxic properties of mutant Notch3 using stable cell lines with inducible expression of either wild-type or two mutants p.R133C and p.C185R. We found that both mutants of Notch3 were prone to aggregation and retained in the endoplasmic reticulum (ER). The turnover rates of the mutated Notch3 proteins were strikingly slow, with half-lives greater than 6 days, whereas wild-type Notch3 was rapidly degraded, with a half-life of 0.7 days. The expression of mutant Notch3 also impaired cell proliferation compared with wild-type Notch3. In addition, cell lines expressing mutant Notch3 were more sensitive to proteasome inhibition resulting in cell death. These findings suggest that prolonged retention of mutant Notch3 aggregates in the ER decreases cell growth and increases sensitivity to other stresses. It is also possible that the aggregate-prone property of mutant Notch3 contributes to a pathogenic mechanism underlying CADASIL.

INTRODUCTION

Cerebral autosomal-dominant arteriopathy with subcortical infarcts and leukoencephalopathy (CADASIL) is the most common hereditary small vessel disease that is characterized by recurrent subcortical ischemic strokes and ultimately vascular dementia (1–5). The pathological hallmark of the disorder comprises a non-amyloid and systemic angiopathy affecting mainly small and medium-size arteries (6,7). These vascular lesions are characterized by degeneration and loss of vascular smooth muscle cells (VSMCs), as well as the abnormal accumulation of granular osmiophilic material (GOM) that is also associated with the extracellular domain of Notch3 (8). CADASIL is caused by missense mutations and small deletions in the *NOTCH3* gene located on chromosome 19p13.1–13.2 (9,10). More than 170 different mutations have been found in families of many ethnic origins (11). Because Notch3 is robustly expressed in VSMCs of the vessel wall (12), VSMCs are the primary target of the pathogenic process in CADASIL.

The *NOTCH* genes, four of which are known to exist, encode highly conserved transmembrane (TM) receptors of about 300 kDa that are involved in cell fate specification during embryonic development (13). The basic structure of the Notch receptor is common to all Notch proteins: the large extracellular domain is composed of a stretch of tandem epidermal growth factor (EGF)-like repeats involved in ligand binding, and the intracellular domain includes Ankyrin/Cdc10 repeats flanked by functional nuclear localization signal sequences. During maturation and activation,

*To whom correspondence should be addressed at: Department of Vascular Dementia Research, National Institute for Longevity Sciences, National Center for Geriatrics and Gerontology, 36-3, Gengo, Morioka, Obu city, Aichi 474-8511, Japan. Tel: +81 562462311; Fax: +81 562468438; Email: watsushi@nils.go.jp
†Present address: Division of Developmental Neuroscience, Center for Translational and Advanced Animal Research (CTAAR), Tohoku University Graduate School of Medicine, 2-1, Seiryo-machi, Aoba-ku, Sendai, Miyagi, Japan.

Notch receptors undergo at least three distinct proteolytic cleavages. Following ligand interaction, the third (S3) cleavage occurs within the TM domain close to the cytoplasmic border by γ-secretase (14), which releases the intracellular domain from the cell membrane, allowing it to translocate to the nucleus and modify the transcription of target genes (15).

Thus far, the mechanisms underlying the pathological alterations in CADASIL remain unclear. CADASIL-causing mutations result in an odd number of cysteine residues in the EGF-like repeats (10). Therefore, the formation of abnormal disulfide bridges has been thought to affect receptor trafficking, processing, specificity for ligand binding and/or signal transduction (10). It remains controversial, however, whether CADASIL mutations affect receptor trafficking and signal transduction. Recent studies have suggested that mutations located in the ligand-binding site can impair signal transduction activity, whereas neither Notch3 processing nor signaling was significantly affected by other mutations outside of the ligand-binding site (16–19). On the other hand, transgenic mice expressing mutant human Notch3 (R90C) exhibited early arterial defects in normal appearing VSMC anchorage onto the adjacent extracellular matrix and cells as well as the VSMC cytoskeleton (20). These changes were followed by the appearance of GOM deposits, suggesting that cell adhesion or the cell–matrix interaction may be affected by mutations in Notch3 and that GOM deposits are not directly involved in the early stages of VSMC abnormalities. Proteomic studies using cultivated VSMCs from a CADASIL patient also revealed differences in the expression levels of proteins involved in protein degradation and folding, indicating that mutant Notch3 causes endoplasmic reticulum (ER) stress and activates the unfolded protein response (UPR) (21). Therefore, it is plausible that mutant Notch3 instigates cytotoxic effects and induces misfolding or aggregation of proteins.

To investigate the toxic effect of mutant Notch3 in culture cells, we established Notch3-inducible human embryonic kidney (HEK) 293 cell lines using the tetracycline (Tet)-on regulatory system. Here, we report that mutants of Notch3 are more prone to form aggregates, which accumulate in the ER, and more resistant to ER-associated degradation (ERAD) than wild-type Notch3. In addition, we conclude that cells expressing mutant Notch3 exhibit impaired proliferation and increased sensitivity to proteasome inhibition resulting in cell death.

RESULTS

Preparation of stable cell lines

To study the role of mutant Notch3 in CADASIL pathogenesis, we first generated cultured human aortic smooth muscle cells (Clonetics AoSMC, Lonza) expressing either wild-type or mutant [arginine 133 to cysteine (p.R133C) or cysteine 185 to arginine (p.C185R)] human Notch3. The expression of Notch3 in VSMC, however, caused excessive cell death as early as 2 days after transfection. Therefore, we established stable HEK293 cell lines in which the expression of Notch3 was inducible using the tetracycline (Tet)-on regulatory system (T-Rex system; Invitrogen). Several cell lines were obtained and at least three cell lines for each construct were selected for subsequent experimentation on the basis of equivalent expression of Notch3 (Fig. 1). Overexpression of either wild-type Notch3 or mutant Notch3 caused a pronounced increase in the expression of the ER-resident protein-folding chaperones GRP78/BiP and ERp72 (Fig. 1). These cell lines were morphologically indistinguishable by light microscopy and exhibited similar doubling rates.

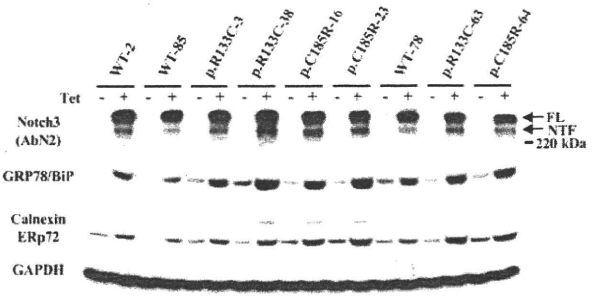

Figure 1. Expression of Notch3 in stable cells by western blot analysis. Cells were incubated with (Tet+) or without (Tet−) tetracycline (2 μg/ml) for 24 h. Cell lysates (30 μg) were prepared and subjected to SDS–gel electrophoresis. Specific proteins were detected using the relevant antibodies. The expression of Notch3 was induced by tetracycline in all cell lines. FL or NTF indicates full length or N-terminal fragment of Notch3, respectively. The same piece of membrane was probed simultaneously with Calnexin and ERp72 antibodies. The data shown are from one representative experiment for nine stable cell lines. The experiment was performed twice and similar results were obtained.

Subcellular localization of Notch3

We determined whether inducible expression of Notch3 altered the intracellular localization of mutant Notch3. The expression of either wild-type Notch3 or mutant Notch3 was induced for 24 h by tetracycline, and cells were then immunostained with Notch3 antibodies and analyzed by light microscopy. As shown in Figure 2A, mutant Notch3 tended to form dot-like aggregates in the perinuclear region of the cytoplasm, and intense immunoreactivity was detected, while only a few cells expressing with wild-type Notch3 contained the aggregates. Quantification of Notch3 immunostaining of stable cell lines revealed that nearly 50% of the mutant Notch3-expressing cells contained the intracellular aggregates. In contrast, wild-type Notch3-expressing cells containing the aggregates accounted for ~15% of the total cells (Fig. 2B).

In further analysis, we determined the precise intracellular localization of Notch3 aggregates by double-immunocytochemistry using two different ER markers (GRP78/BiP and calnexin) and a Golgi complex marker (58 K protein). In cells expressing either wild-type or mutant Notch3, most of the aggregates were colocalized with GRP78/BiP and calnexin (Fig. 3). Golgi 58 K immunoreactivity, however, was not apparent in the aggregates (Supplementary Material, Fig. S1), indicating that the Golgi complex was not involved. These observations indicated that mutant Notch3 was prone to aggregation and accumulated in the ER.

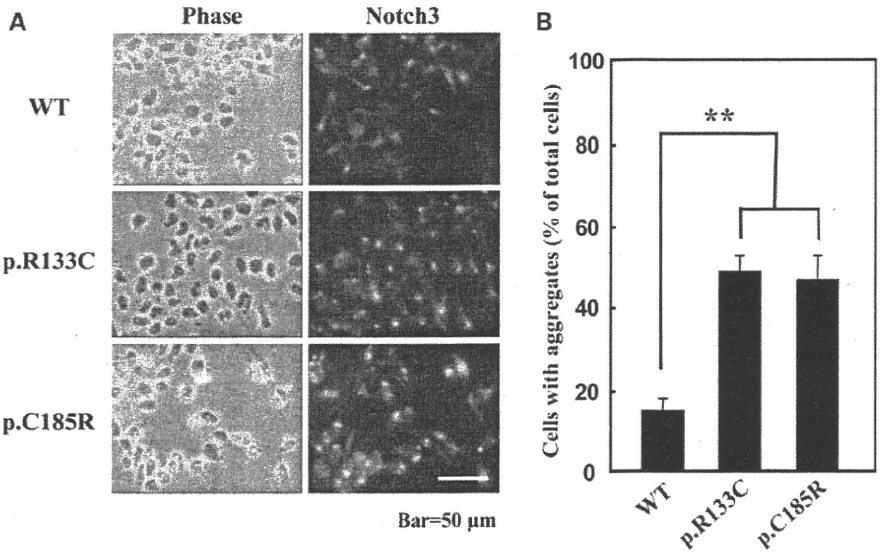

Figure 2. Immunocytochemical analysis of Notch3 in stable cells. Stable cells were treated with tetracycline (2 μg/ml) for 24 h and then stained with the anti-Notch3 antibody. (**A**) Phase contrast (left) and fluorescence (right) microscopy images were captured directly from the culture dish. This shows dot-like aggregates in the immunopositive cells. The data shown are from one representative experiment for three stable cell lines (WT-2, p.R133C-63 and p.C185R-16). The experiment was performed twice using all stable cell lines and similar results were obtained. Scale bar, 50 μm. (**B**) Cells with aggregates were quantified manually by counting cell numbers in phase contrast and immunofluorescence microscopy images and scored as the percentage of the total number of cells. Mutant Notch3 tended to form aggregates in the cytoplasm. Values represent means ± SD of data from four independent images of each stable cell line. $^{**}P < 0.01$ relative to wild-type Notch3-expressing cells.

Clearance of wild-type and mutant Notch3

The results of the immunostaining described above demonstrated that mutant Notch3 formed aggregates that are retained in the ER. Many studies have reported that mutations in proteins often cause structural alterations and result in misfolded proteins that are sequestered by ER chaperones for refolding and trafficking, before ultimately being eliminated by the ERAD system (22–28). Therefore, we determined the degradation rates of wild-type Notch3 and mutant Notch3 using pulse-chase experiments. Stable cells were treated with tetracycline for 24 h, radiolabeled for 2 h and then chased for 1–2 days in medium containing unlabeled methionine and cysteine. The labeled proteins were immunoprecipitated using an anti-Notch3 antibody. As shown in Figure 4, labeled wild-type Notch3 rapidly disappeared within 2 days and its half-life was determined to be ~0.7 days. In contrast, >70% of labeled mutant Notch3 proteins were still detectable after 2 days of chase (Fig. 4B); the half-lives of the mutants were estimated to be ~9 days for p.R133C and ~6 days for p.C185R from the slopes of the relative intensity curves. This slower degradation of mutant Notch3 was assayed by immunostaining stable cells (Fig. 5). The cells were treated with tetracycline for 24 h and then cultured in medium without tetracycline for 2 days. As expected, dot-like aggregates in the immunopositive cells of wild-type Notch3 quickly disappeared, whereas mutant aggregates did not show any discernible reduction up to 2 days. Quantitative analysis revealed that cell numbers with mutant aggregates did not appear to change for 2 days after turning off expression of the mutant Notch3. These results were confirmed by quantitative western blot analysis of stable cell lines (Supplementary Material, Fig. S2), although the amounts of mutant Notch3 (p.R133C) increased slightly at 1 day. It was also noted that wild-type Notch3 was almost entirely degraded within 2 days after arresting its expression. Thus, the aggregates of mutant Notch3 were highly resistant to degradation by the ERAD system.

Mutant Notch3 binds to ER chaperones

It has been reported that misfolded or aggregated proteins that are retained in the ER are associated with ER chaperones (22–27). We examined whether mutant Notch3 interacts with certain ER chaperones. Cell lysates were subjected to immunoprecipitation with an anti-Notch3 antibody, and the immunoprecipitated complexes were analyzed by western blotting. As shown in Figure 6, the chaperone calnexin co-immunoprecipitated with mutant Notch3 but not with wild-type Notch3, indicating that mutant Notch3 interacted exclusively with calnexin. On the other hand, GRP78/BiP co-immunoprecipitated with both the wild-type and mutant Notch3, although the amount of GRP78/BiP was higher in the mutant Notch3 immunoprecipitated samples than in the wild-type sample. The other chaperones, ERp72 and PDI, were not detected in immunoprecipitated samples of wild-type or mutant Notch3. These findings suggest that aggregation of mutant Notch3 may lead to prolonged association with calnexin, leading to retention of the aggregates in the ER.

Expression of mutant Notch3 inhibits cell proliferation

We further determined whether expression of mutant Notch3 affects cell viability. Figure 7A shows the typical growth